Measurement of Collector-Base Junction Avalanche Multiplication Effects in Advanced UHV/CVD SiGe HBT's

Guofu Niu, *Member, IEEE,* John D. Cressler, *Senior Member, IEEE,* Shiming Zhang, *Student Member, IEEE,*
Usha Gogineni, *Student Member, IEEE,* and David C. Ahlgren

***Abstract*—This paper presents measurements of the avalanche multiplication factor ($M-1$) in SiGe HBT's using a new technique capable of separating the avalanche multiplication and Early effect contributions to the increase of collector current with collector-base bias, as well as allowing safe measurements at practical current densities. The impact of collector doping, current density, Ge profile, and operation temperature are reported for the first time using measured and simulated results from a production-quality UHV/CVD SiGe HBT technology. Limitations of the technique in the presence of significant self-heating are discussed. By turning on the secondary hole impact ionization, we revealed the difference in impact ionization between strained SiGe and Si in the presence of the "dead space" effect. Despite its smaller bandgap, the compressively strained SiGe layer shows an apparent decrease in the secondary hole impact ionization rate compared to Si.**

***Index Terms*—Avalanche multiplication, "Dead space" effect, Early effect, HBT, impact ionization, nonequilibrium transport, SiGe.**

I. INTRODUCTION

To realize optimum performance, SiGe HBT's are typically designed with heavily doped implanted collectors. For practical circuits operating at either high collector current density (J_C) or high collector-base bias ($V_{\rm CB}$), avalanche multiplication is an important effect that must be accurately measured and modeled. In digital applications, the avalanche multiplication factor ($M-1$) determines the breakdown voltage and the base current reversal voltage, which in turn determines the maximum power supply for stable logic operation [1], [2]. In analog applications, avalanche multiplication seriously degrades the output resistance of an amplifier [3]. In critical RF circuits such as power amplifiers (PA) and low noise amplifiers (LNA), the collector-base junction avalanche multiplication degrades the linearity of the circuit because of the resulting strong nonlinear feedback from the output (collector) to the input (base) [4], [5]. This is particularly the case for state-of-the-art high-performance transistors featuring high collector doping. The accuracy of avalanche multiplication models in either the traditional SPICE modeling [6] or more complicated mixed-mode device/circuit simulation [5] is critical to the device design of high linearity LNA and PA circuits.

The avalanche multiplication factor in SiGe HBT's has been recently measured in [7] using a forced-I_E technique that allows a safe extraction of the multiplication factor at much higher bias and currents than with the conventional forced-$V_{\rm BE}$ method [2]. The technique in [7], however, did not explicitly account for the Early effect, which makes the results inaccurate at low $V_{\rm CB}$, as shown below. We present here an improved $M-1$ extraction technique capable of properly accounting for the Early effect, as well as a novel method to separate the avalanche multiplication and Early effect contributions to J_C. This separation is important for both accurate circuit modeling and a basic physical understanding of device operation, because of their very different impact on the base and emitter currents, as will be detailed below. We present in this work the measured results of multiplication factor from a production-quality UHV/CVD SiGe HBT technology. Guided by numerical simulation, we also explore the difference in avalanche multiplication rate by holes between SiGe and Si by turning on the secondary hole impact ionization.

II. DEVICE TECHNOLOGY AND MEASUREMENT SETUP

The devices were fabricated using a self-aligned epitaxial-base technology [8]. Fig. 1 shows a schematic cross section of the device. The SiGe base is formed in an ultra-high-vacuum/chemical vapor deposition (UHV/CVD) low-temperature epitaxy (LTE) system. Polysilicon deposited over the field oxide during the LTE serves as the extrinsic base contact. Polysilicon-filled, closed-bottom, deep trenches isolate adjacent subcollectors, and the field oxide is fabricated using a planar shallow trench process. For standard devices in the technology, the intrinsic collector was formed by a double implantation to realize high performance. Representative vertical doping and Ge profiles of the standard SiGe HBT are shown in Fig. 2. For RF power applications, devices with a higher breakdown voltage were fabricated on the same wafer by leaving out one or both of the collector implantations [9]. Thereafter we will refer to the standard device with a double collector implant, the single collector implant device, and the

---

Manuscript received October 15, 1998; revised December 14, 1998. The review of this paper was arranged by Editor J. N. Hollenhorst. This work was supported by J. D. Cressler's IBM University Partner Award.

G. Niu, J. D. Cressler, S. Zhang, and U. Gogineni are with the Alabama Microelectronics Science and Technology Center, Electrical Engineering Department, Auburn University, AL 36849 USA.

D. C. Ahlgren is with IBM Microelectronics, Hopewell Junction, NY 12533 USA.

Publisher Item Identifier S 0018-9383(99)03516-9.

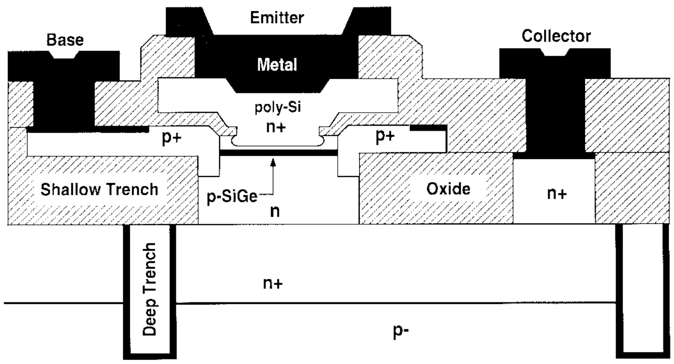

Fig. 1. Schematic cross section of the UHV/CVD SiGe HBT used in this investigation.

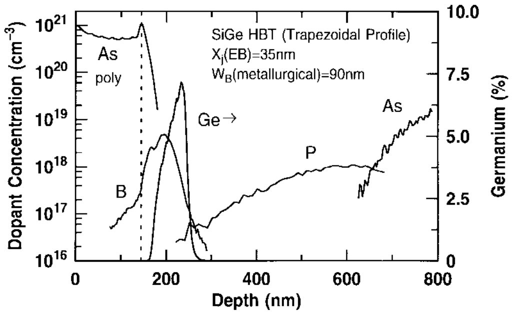

Fig. 2. Representative doping and Ge profiles of a UHV/CVD SiGe HBT with double collector implantation (the high N_C device).

TABLE I

SUMMARY OF THE ELECTRICAL CHARACTERISTICS OF THE HIGH, MEDIUM, AND LOW N_c SiGe HBT'S. THE DEVICE HAS TWO 0.5×20 μm^2 EMITTER STRIPES

	High N_c	Medium N_c	Low N_c
Peak β	110	95	85
Peak f_T (GHz)	51	33	16
Peak $f_{\max}$ (GHz)	64	40	20
R_b (Ω)@ I_c =10 mA	8.9	10.2	10.7
BV_{CEO} (V)	3.3	5.3	7.5

no collector implant device as the high, medium and low collector doping ($\mathrm{N_C}$) SiGe HBT's, respectively.

DC characteristics were measured on-wafer using an HP4155 with a probe station capable of operating from 80 to 300 K, and ac characteristics were measured on-wafer using an HP8510C network analyzer. Key electrical characteristics, including the peak current gain (β), peak cutoff frequency (f_T), peak maximum oscillation frequency $(f_{\max})$, the base resistance (R_b), and open-base breakdown voltage $(\mathrm{BV_{CEO}})$ are summarized in Table I for a 0.5 (emitter width) $\times$ 20 (emitter length) $\times$ 2 (number of emitter stripes) μm^2 device with different collector doping. Two-dimensional (2-D) numerical simulations using MEDICI [10] were performed to help understand experimental observations. The coefficients of physical models such as the bandgap narrowing (BGN) parameters in SiGe and Si used in the simulations were calibrated such that both the dc and ac characteristics were reproduced from simulation with reasonable accuracy. Vertical SIMS doping and Ge profiles were used in the simulation, and the lateral transition between the extrinsic and intrinsic base was determined by best fitting the measured and simulated base resistance [11].

III. MEASUREMENT TECHNIQUE

We first derive the theoretical equations for $M-1$ extraction under a fixed emitter current measurement setup including the Early effect, which was not taken into account in our earlier technique [7]. Although the measurement of $M-1$ at fixed emitter current had been previously used in the literature [12], [13], the equation for $M-1$ calculation under the conventional fixed base-emitter voltage setup [2] was used

$$M-1=\frac{\Delta I_s}{I_C-\Delta I_B}$$
$$\Delta I_B=I_B(V_{\mathrm{CB}}=0)-I_B(V_{\mathrm{CB}}). \qquad (1)$$

The use of the fixed base-emitter voltage $M-1$ equation for fixed emitter current measurement setup is obviously incorrect because the base-emitter voltage decreases due to the Early effect, as confirmed by measurement. As a result, the base current reduction term $I_B(V_{\mathrm{CB}}=0)-I_B(V_{\mathrm{CB}})$ is no longer purely due to avalanche multiplication, but instead is a mixed result of the base-emitter voltage decrease which itself reduces I_B, and the avalanche multiplication. Consequently, $M-1$ is overestimated when the fixed base-emitter voltage equation was used for fixed emitter current measurement setup. The correct $M-1$ equation for the fixed emitter current measurement setup is derived below, followed by experimental verification.

A. Theoretical Analysis

To measure $M-1$, the collector-base voltage (V_{CB}) is swept at a fixed emitter current (I_E), and the emitter-base voltage (V_{BE}) is recorded. Because of the Early effect, V_{BE} decreases with increasing V_{CB}, thus decreasing the base current injected into the emitter, and hence increasing the initial current for avalanche multiplication (I_{init}). To calculate the multiplication factor, we first need to determine the component of emitter current that recombines with holes before reaching the collector-base junction so as to determine the initial electron current I_{init} for avalanche multiplication. For modern transistors, hole injection into the emitter is far more significant than neutral base recombination, and therefore one has

$$I_C=MI_{\mathrm{init}}+I_{\mathrm{CBO}} \quad I_{\mathrm{init}}=I_E-I_B(V_{\mathrm{BE}})|_{V_{\mathrm{CB}}=0} \qquad (2)$$

where I_{CBO} is the collector-base leakage current with a floating emitter. The base current measured under $V_{\mathrm{CB}}=0$ for a V_{BE} value recorded during the V_{CB} sweep was used as the component of emitter current that recombines with holes before reaching the collector-base junction. The essence of the assumption is that for a virtual transistor without avalanche multiplication, the base current is solely determined by V_{BE}. This assumption is well satisfied for today's Si and SiGe transistors with narrow base and shallow emitter, in which the hole injection into the emitter is far more significant than neutral base recombination current, even for devices with evenly substantial neutral base recombination [14]. For transistors in which neutral base recombination dominates the base current, the base doping needs to be much higher than the collector doping to satisfy this assumption. In the latter case, the sweep in $V_{\rm CB}$ does not significantly affect the neutral base boundary because most of the depletion occurs on the collector side, and therefore does not affect the neutral base recombination current. This assumption in fact is also made in the conventional fixed-$V_{\rm BE}$ multiplication factor measurement technique [2].

The multiplication factor $M-1$ is then extracted from (2) as

$$M-1=\frac{I_C-I_{\rm CBO}}{I_E-I_B(V_{\rm BE})|_{V_{\rm CB}=0}}-1. \tag{3}$$

Next, we extract the Early effect factor $F_{\rm Early}$ which is related to the initial current $I_{\rm init}$ by the following definition:

$$I_{\rm init}=I_C(V_{\rm BE})|_{V_{\rm CB}=0}\times F_{\rm Early}. \tag{4}$$

Another description of this equation is that the electron current at the collector-base junction boundary increases with $V_{\rm CB}$ by a factor of $F_{\rm Early}$. The $F_{\rm Early}$ factor is related to the conventional Early voltage (V_A) through $F_{\rm Early}=1+V_{CE}/V_A$. Experimentally it has been established that the traditional "Early voltage" approach to the modeling of Early effect is not sufficient to model the output resistance for analog circuits [15]. The determination of the Early voltage can be very difficult in practice because: 1) the output I_C-V_{CE} curve usually deviates from linear, and 2) the intersection of the extrapolated I_C curve with V_{CE} axis is a function of bias [16]. The technique here allows a direct measurement of the Early effect factor as a function of bias. From (2) to (4), one has

$$F_{\rm Early}-1=\frac{I_E-I_B(V_{\rm BE})|_{V_{\rm CB}=0}}{I_C(V_{\rm BE})|_{V_{\rm CB}=0}}-1. \tag{5}$$

A separate measurement of I_B and I_C with $V_{\rm CB}=0$ at the $V_{\rm BE}$ values recorded during the fixed-I_E $V_{\rm CB}$ sweep determines $M-1$ and $F_{\rm Early}-1$ from (3) and (5).

One may ask why we need to separate the Early effect and avalanche multiplication effect if they both have the same impact on collector current. To answer this, consider a transistor biased at certain $V_{\rm BE}$, and now imagine increasing the collector bias. The Early effect results in an increase in both the collector current density (J_C) and the emitter current density (J_E), with no change in the base current density (J_B) for a transistor without neutral base recombination. Physically, the minority carrier distribution in the base is changed, which results in an increase in both the emitter current and the collector current. Avalanche multiplication, however, by its very nature, results in not only an additional increase in J_C, but also a decrease in J_B by **the same amount**. The emitter current J_E, however, is not affected. In practical circuit operation, this creates a strong nonlinear feedback from the output to the input for common-emitter operation [5], and is thus important.

B. Experimental Verification

Fig. 3 shows the Gummel characteristics of a typical 0.5×2.5 μm^2 high-N_C SiGe HBT used in this investigation. The left axis shows the collector and base currents, and the right axis shows the current gain. Fig. 4 compares the multiplication factor $M-1$ versus $(V_{\rm CB})$ extracted using the conventional forced-$V_{\rm BE}$ technique [2], the forced-I_E technique introduced in [7], and the new forced-I_E technique presented here. With Early effect correction, more accurate results at low $V_{\rm CB}$ are obtained and the advantage of safe extraction at high $V_{\rm CB}$ and J_C is retained. Catastrophic thermal breakdown occurs when the conventional technique is used, due to the positive feedback of self-heating on I_E at fixed $V_{\rm BE}$.

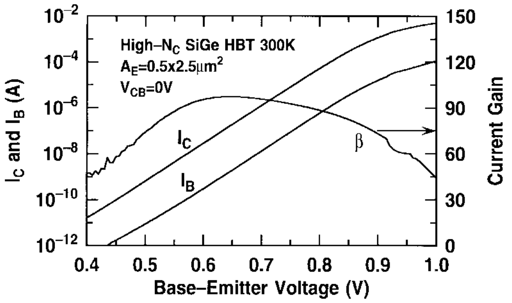

Fig. 3. Gummel characteristics of a typical high-N_C SiGe HBT. The left axis shows the collector and base currents, and the right axis shows the current gain.

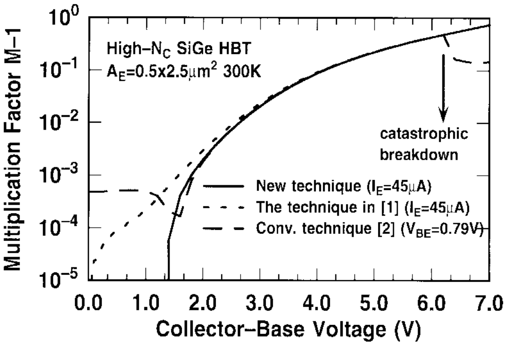

Fig. 4. Measured $(M-1)$–$(V_{\rm CB})$ using the conventional forced-$V_{\rm BE}$ technique, the forced-I_E technique proposed in [1], and the new technique proposed in this work.

Fig. 5 shows the measured $V_{\rm BE}$ change during the $V_{\rm CB}$ sweep for two different emitter currents. Clearly $V_{\rm BE}$ decreases with increasing $V_{\rm CB}$, because a higher $V_{\rm CB}$ leads to a higher initial current due to the Early effect. When $V_{\rm CB}$ increases, $V_{\rm BE}$ has to decrease to maintain the total amount of I_E. The amount of $V_{\rm BE}$ change during the $V_{\rm CB}$ sweep under fixed-I_E is a direct measure of the Early effect. Fig. 6 shows the $F_{\rm Early}-1$ and $M-1$ corresponding to Fig. 5. The measured Early effect factor is larger at higher bias current, and the measured multiplication factor is about the same for these two bias currents. Possible reasons for the observed current dependence include the self-heating induced collector current increase, and the free carrier induced neutral base boundary shift. The I_C increase due to Early effect is considerably larger than that due to avalanche multiplication at $V_{\rm CB}<2$ V. At low $V_{\rm CB}$ values, there is physically no impact ionization taking place because the maximum possible kinetic energy in the absence of scattering is less than the threshold for impact ionization. The values of $M-1$ extracted are thus due to the finite amount of collector-base conductance due to neutral base

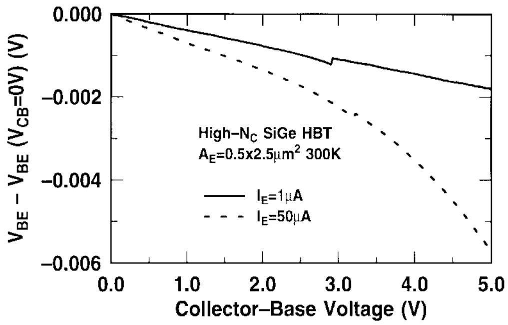

Fig. 5. $V_{\rm BE}$ change during the fixed-I_E $V_{\rm CB}$ sweep for $I_E = 1$ and 50 μA.

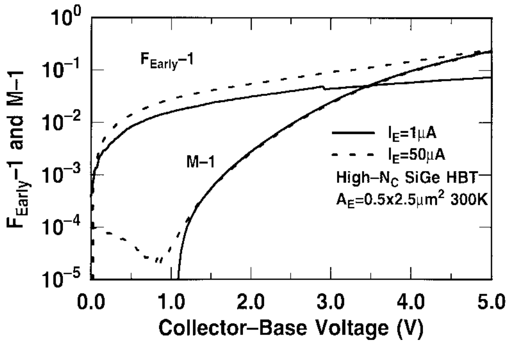

Fig. 6. Measured $M-1$ and $F_{\rm Early}-1$-($V_{\rm CB}$) from (3) and (5) for $I_E = 1$ and 50 μA.

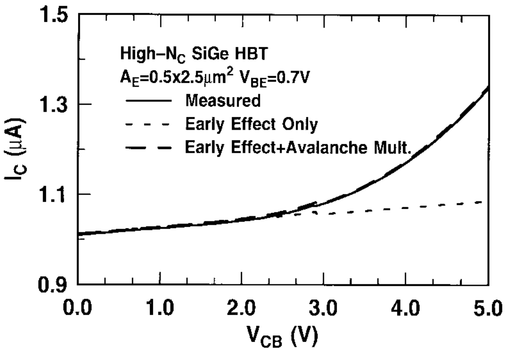

Fig. 7. Comparison of I_C–$V_{\rm CB}$ at fixed $V_{\rm BE}$ of 0.7 V calculated from the measured $F_{\rm Early}$ and $M-1$ at fixed I_E using (6) with directly measured I_C–$V_{\rm CB}$ at $V_{\rm BE}$ of 0.7 V. In this manner, the individual contributions of Early effect and avalanche multiplication to the increase of collector current can be separated.

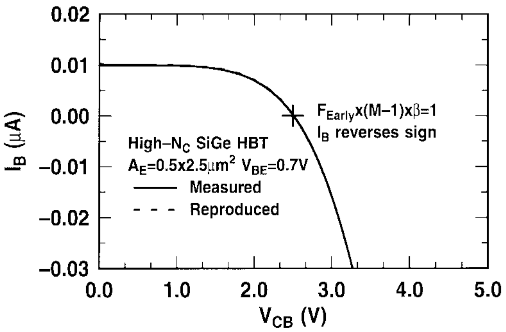

Fig. 8. Comparison of I_B– $V_{\rm CB}$ at fixed $V_{\rm BE}$ of 0.7 V calculated from the measured $F_{\rm Early}$ and $M-1$ at fixed I_E using (7) with directly measured I_B–$V_{\rm CB}$ at $V_{\rm BE}$ of 0.7 V.

recombination. This limitation is common to all the existing $M-1$ extraction methods, and for this very reason, the $M-1$ below $V_{\rm CB}$ of 1 V is usually not plotted in measurements using the conventional fixed-$V_{\rm BE}$ technique [2].

For further verification, we apply the $F_{\rm Early}-1$ and $M-1$ measured under forced-I_E operation to reproduce the forced-$V_{\rm BE}$ output I_C

$$I_C(V_{\rm BE})|_{V_{\rm CB}} = I_C(V_{\rm BE})|_{V_{\rm CB}=0} \times F_{\rm Early} \times M. \qquad (6)$$

The results are shown in Fig. 7, and the reproduction agrees well with the values directly measured under forced-$V_{\rm BE}$ operation. The base current decreases with increasing $V_{\rm CB}$ by an amount equal to the avalanche multiplication generated electron current

$$\begin{aligned} I_B(V_{\rm BE})|_{V_{\rm CB}} =& I_B(V_{\rm BE})|_{V_{\rm CB}=0} - I_C(V_{\rm BE})|_{V_{\rm CB}=0} \\ & \times F_{\rm Early} \times (M-1). \end{aligned} \qquad (7)$$

The avalanche multiplication induced base current reduction equals $I_C(V_{\rm BE})|_{V{\rm CB}=0} \times F_{\rm Early} \times (M-1)$ where $I_C(V_{\rm BE})|_{V_{\rm CB}=0} \times F_{\rm Early}$ gives the initial current for avalanche multiplication. The open emitter current $I_{\rm CBO}$ in these devices is extremely small (pA level) and therefore can be safely neglected. The calculated base current change during the forced-$V_{\rm BE}$ sweep from (7) using the measured $F_{\rm Early}$ and $M-1$ extracted from the forced-I_E sweep agrees well with the values directly measured under forced-$V_{\rm BE}$ sweep, as shown in Fig. 8. The individual contributions of Early effect and avalanche multiplication are clearly and properly revealed in this way for the first time. Note that the base current decreases monotonically with increasing $V_{\rm CB}$, which implies that self-heating is not significant in this case as far as its effect on the base current reduction is concerned. In the presence of significant self-heating, the junction temperature increases with increasing $V_{\rm CB}$, which would result in a local increase of base current at low $V_{\rm CB}$ when measured under forced-$V_{\rm BE}$ mode. Special care needs to be taken to extract $M-1$ at high current densities, as discussed below. From (7), we can easily determine the condition for the base current to reverse its sign

$$\beta|_{V_{\rm CB}=0} \times F_{\rm Early} \times (M-1) = 1. \qquad (8)$$

The base current is positive below the base current reversal voltage at which (8) holds, and becomes negative above this voltage.

IV. DISCUSSION

A. Effects of Self-Heating

At the high current densities and high $V_{\rm CB}$ which may cause significant self-heating, substantial errors may result from using the proposed technique as is. The difficulty lies in the inaccurate estimation of the emitter component that recombines with holes before reaching the collector-base space charge region (CB-SCR). Without self-heating, this current component was determined using the base current measured at the $V_{\rm BE}$ values recorded during the fixed-I_E $V_{\rm CB}$ sweep. With significant self-heating, the hole injection into the emitter depends on not only $V_{\rm BE}$, but also $V_{\rm CB}$ through the junction temperature. A simple fix, however, exists if the $M-1$ is higher than the reciprocal of β. In actual measurements, one can identify this by comparing the measured I_C/I_E-1 with the reciprocal of β. The initial current $I_{\rm init}$ can then be approximated by the emitter current I_E, and I_C/I_E-1 can be approximated as $M-1$. Insight can be gained by expressing M in a different manner

$$\begin{aligned} M &= \frac{I_C}{I_E - I_B(V_{\rm BE})|_{V_{\rm CB}=0,T(V_{\rm CB})}} \\ &= \frac{I_C}{I_E - (1 - 1/\beta(V_{\rm BE})|_{V_{\rm CB},T(V_{\rm CB})}} \\ &\approx \frac{I_C}{I_E}\left(1 + 1/\beta(V_{\rm BE})|_{V_{\rm CB},T(V_{\rm CB})}\right). \end{aligned} \tag{9}$$

When $(I_C/I_E) \gg 1 + 1/\beta(V_{\rm BE})|_{V_{\rm CB},T(V_{\rm CB})}$, one can safely neglect the $1/\beta(V_{\rm BE})|_{V_{\rm CB},T(V_{\rm CB})}$ term. For instance, if the current gain is around 100, $(I_C/I_E) = 1.1$, the M value obtained by neglecting the $1/\beta(V_{\rm BE})|_{V_{\rm CB},T(V_{\rm CB})}$ term is 1.1. This is a good approximation to its actual value of $1.1 \times (1 + 1/100) = 1.111$. $1/\beta(V_{\rm BE})|_{V_{\rm CB},T(V_{\rm CB})}$ in principle is a function of the current density and $V_{\rm CB}$ due to its junction temperature and Early effect dependence. However, as long as the measured I_C/I_E is far larger than $1/\beta(V_{\rm BE})|_{V_{\rm CB},T(V_{\rm CB})}$, one can simply take I_E as the initial current, and take I_C/I_E-1 as $M-1$, with little error introduced. In other words, self-heating may either increase or decrease the current gain, but as long as the gain is high enough, and for the high $V_{\rm CB}$ region where $M-1$ is large, a very good approximation of the actual $M-1$ is still obtained. The obtained values, however, are the values of $M-1$ at the junction temperature which itself is a function of bias, because $M-1$ is a function of the lattice temperature. The approximation obviously cannot be made in situations where $M-1$ is smaller than $1/\beta$. In practical devices, one can utilize the above approximation in situations where $(I_C/I_E) \gg 1 + 1/\beta(V_{\rm BE})|_{V_{\rm CB},T(V_{\rm CB})}$ is observed in the measurement. In our devices, however, we did not observe $(I_C/I_E) \gg 1 + 1/\beta(V_{\rm BE})|_{V_{\rm CB},T(V_{\rm CB})}$ at high current density, because the $M-1$ factor decreases with increasing current density, due to the Kirk effect [17]. The compensation of depletion charges by free carriers reduces the electric field in the CB-SCR, and hence reduces $M-1$, as we will show below. Therefore, the measurement of $M-1$ at high current densities could be even more difficult for a low N_C device in which the Kirk effect is strong, because of its intrinsically lower value of $M-1$, as confirmed by the measurement below. $(I_C/I_E) \gg 1 + 1/\beta(V_{\rm BE})|_{V_{\rm CB},T(V_{\rm CB})}$ can therefore be expected to occur in future devices with higher collector doping than the high-N_C devices used in this work. In that case, self-heating can be well tolerated by using the above approximation. Another indication of (9) is that a high current gain transistor is desirable from the viewpoint of measuring the multiplication factor.

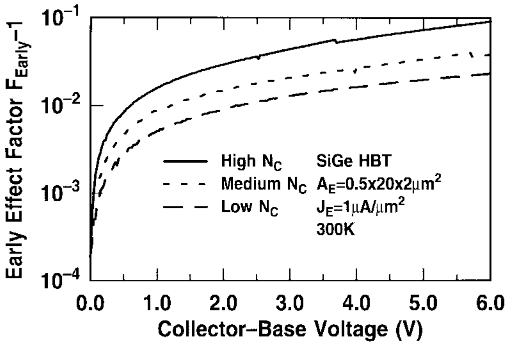

Fig. 9. Early effect factor $(F_{\rm Early} - 1)$–$V_{\rm CB}$ for three different collector doping profiles.

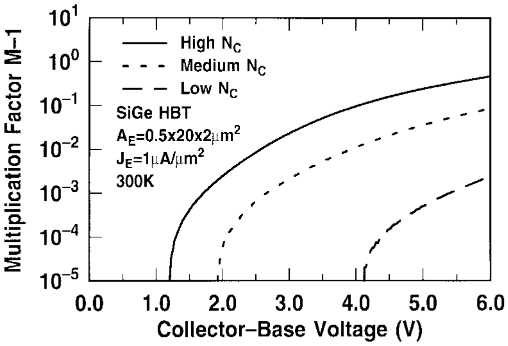

Fig. 10. Multiplication factor $(M - 1)$–$V_{\rm CB}$ for three different collector doping profiles.

B. Impact of Collector Doping

Figs. 9 and 10 show the Early effect factor $F_{\rm Early}-1$ and multiplication factor $M-1$–$V_{\rm CB}$ for three devices with different collector doping fabricated on the same wafer ($\mathrm{BV_{CEO}} = 3.3$, 5.3, and 7.5 V for high, medium and low N_C, respectively). The Early effect is more pronounced for higher collector doping due to its larger CB junction capacitance, and $M-1$ dramatically decreases at lower collector doping due to its smaller CB junction electric field, as expected. The fact that there is no avalanche multiplication at $V_{\rm CB}$ of 3.0 V (3.7 eV total potential energy drop across CB-SCR considering a 0.7 V built-in potential) in the low-N_C device strongly suggests that the kinetic energy of the electrons never reaches the threshold for avalanche multiplication, despite the large total potential drop. Consequently, in addition to the sufficiently high collector voltage drop, the occurence of impact ionization requires the peak field to exceed a certain critical value, below which the kinetic energy of the electrons is always lost before reaching the threshold to create an electron-hole pair. The strong field also needs to expand in the CB-SCR for a certain distance so that "lucky" electrons can gain enough energy to create an electron-hole pair.

C. Impact of Current Density and High Current Limitations

For RF power amplifier applications, the devices are usually biased at high current density and high collector bias. Fig. 11 shows the $M-1$ versus the emitter current density J_E for devices with different collector doping levels. The compensation

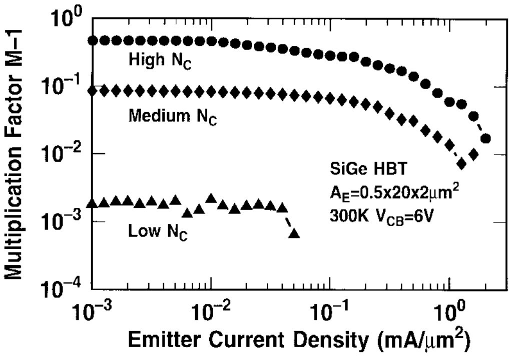

Fig. 11. Multiplication factor $M - 1$ versus emitter current density at $V_{\rm CB} = 6$ V for three different collector doping profiles. At a current density from 0.1 to 1.0 mA/μm^2 where RF amplifiers are typically operated, $M - 1$ is clearly different from its low current density value, indicating the importance of measurement at high current densities.

of charges in the CB space charge region (SCR) by free carriers reduces the effective doping and electric field, thus decreasing $M - 1$ at higher (practical) J_E [2]. The $M - 1$ factor at high current density is small compared to the reciprocal of the current gain (around 100), and was not observed at high current density, for which we can make very good approximations of $M - 1$ as discussed earlier. Fig. 12 shows the measured cut-off frequency as a function of the collector current density for the three collector dopings. For the high and medium N_C devices, the $M - 1$ in the current density range of 0.1–1.0 mA/μm^2, at which SiGe HBT's have optimum frequency response (see Fig. 12), is considerably smaller than its low J_E values, demonstrating the importance of $M - 1$ measurements at these practical operational current densities. This also suggests that $M - 1$ should be modeled as a function of bias current density in RF circuit simulation to accurately predict the nonlinear distortion behavior. For circuit applications such as RF amplifiers, the current densities below the value where the cutoff frequency starts to fall off are of interest. At higher current densities, base push-out occurs, and self-heating effect can be pronounced, making the base current without impact ionization dependent on the collector-base bias, and thus invalidating the fundamental assumption underlying all of the existing extraction methods that the base current without avalanche multiplication is independent of the collector-base bias. The distributed nature of the base recombination current in the CB-SCR also makes the estimation of the initial current inaccurate in this regime.

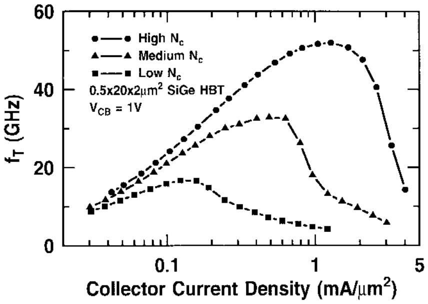

Fig. 12. Measured cut-off frequency versus collector current density at $V_{\rm CB} = 1$ V for the three collector doping profiles.

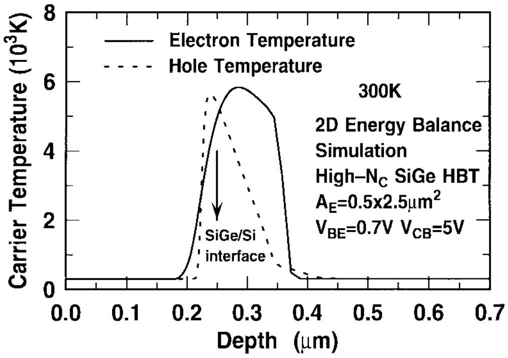

Fig. 13. Simulated depth profile of carrier temperatures at $V_{\rm BE} = 0.7$ V, $V_{\rm CB} = 5$ V taken from the emitter center.

D. Impact of SiGe

Previous studies [8] have shown that the unavoidable SiGe in the CB-SCR of a SiGe HBT does not inadvertently affect $M - 1$, because of the "dead space" effect [18]. The peak electron energy position is deeper in the Si region, thus impact ionization occurs mostly in the silicon region, resulting in the same $M - 1$ for both SiGe and Si devices [7], [8]. A logical question is whether we can measure the avalanche multiplication factor in strained SiGe so as to know how the avalanche multiplication effect changes in SiGe compared to Si. The answer is potentially useful for understanding avalanche multiplication in future pnp SiGe HBT's which require a deeper grading of SiGe into the collector. We propose here to reveal the difference in avalanche multiplication effects in SiGe and Si by observing the multiplication factor at the onset of secondary hole avalanche multiplication. Electrons are accelerated toward the collector side of the CB-SCR, while holes are accelerated toward the base side of the CB-SCR. Consequently hot holes are populated at the base side of the CB-SCR. If the peak hole energy lies in the portion of the CB-SCR where Ge content peaks, we should be able to distinguish the impact ionization by hot holes in SiGe and Si. For this purpose, we performed 2-D numerical simulation using the energy transport advanced application module of MEDICI [10]. Although MEDICI does not have a particular model for the energy transport in strained SiGe, we expect the resulting hole temperature distribution to be useful in at least determining where the peak hole energy lies. The simulated results in Fig. 13 indeed show that the peak hole energy position lies in the region where Ge content peaks in these devices.

Next we measure the multiplication factor up to very high $V_{\rm CB}$ to turn on the secondary hole impact ionization [19]. Electrons get accelerated across the CB-SCR, and generate secondary electron-hole pairs at the end of the CB-SCR. The secondary electrons are collected by the collector, and the secondary holes drift back toward the base side of the CB-SCR. During the drift process, these secondary holes gain energy, and create electron-hole pairs at the base end of the CB-SCR. The above description is a simplified picture of the real process which involves self-consistent solution of the

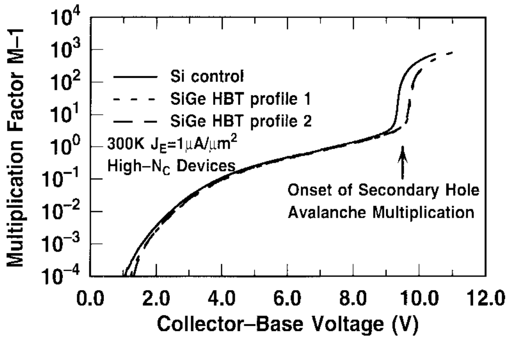

Fig. 14. Multiplication factor $(M-1)$–$V_{\rm CB}$ comparison between SiGe HBT's with different Ge profile and Si control.

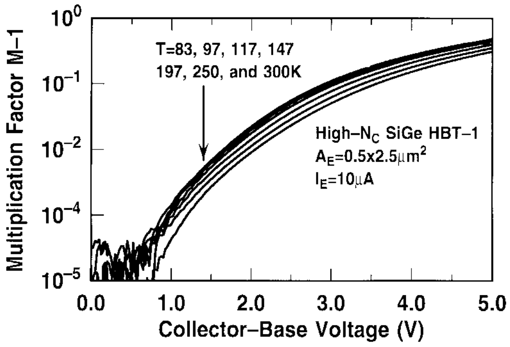

Fig. 15. Multiplication factor $(M-1)$–$V_{\rm CB}$ at various temperatures for a typical SiGe HBT.

transport equation. The signature for secondary hole impact ionization is an abrupt increase of the avalanche multiplication factor [19]. Fig. 14 shows the measured results up to $V_{\rm CB}$ of 12 V in two SiGe HBT's with slightly different Ge grading into the collector, and an identically processed Si control device. The $M-1$ in SiGe HBT's and silicon control are nearly identical at $V_{\rm CB} < 9$ V due to the "dead space" effect. However, in contrast to $V_{\rm CB} < 9$ V, the Si and SiGe devices show a clear difference in $M-1$ at higher $V_{\rm CB}$. When the contributions of impact ionization by secondary holes become significant, as indicated by the dramatic increase in $M-1$. A higher onset voltage for the secondary hole impact ionization and a smaller value of $M-1$ are observed in the SiGe HBT. The result suggests that despite the smaller bandgap of SiGe, the impact ionization rate by holes in the strained SiGe is smaller than in Si, which could be caused by the higher impact ionization threshold due to the in-plane strain. It had been theoretically shown in [20] that the threshold for impact ionization is dramatically increased if a layer is compressively strained without reducing its bandgap. An increase of impact ionization threshold was later experimentally observed in a compressive strained layer with a wider bandgap [21]. Our experimental results in the strained SiGe layer suggest that the threshold for impact ionization can be increased in a compressively strained layer even if the bandgap is reduced. This is indeed good news for hetero-structure MODFET and MOSFET utilizing strained SiGe channel. A very safe extraction up to $V_{\rm CB}$ of 12 V and $M-1$ of 10^3 is easily achieved using the new technique presented in this work.

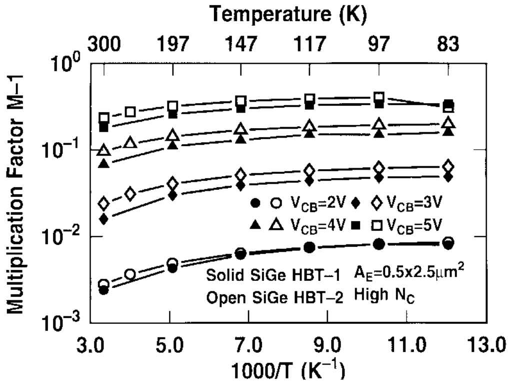

Fig. 16. Multiplication factor $M-1$ versus 1000/T at various $V_{\rm CB}$'s for two SiGe HBT's with different Ge profiles. In contrast to previous observations of an exponential increase in $M-1$ with cooling, we observe here a reduced temperature dependence of $M-1$ with cooling, particularly below 147 K, in the devices under study.

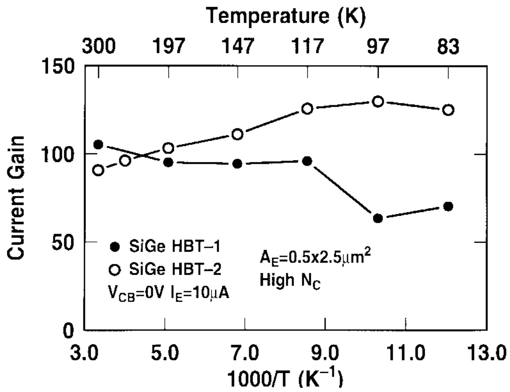

Fig. 17. Current gain versus 1000/T for two SiGe HBT's with different Ge profiles.

E. Low Temperature Operation

Low temperature operation of electronics system has been an active research area for many years. The SiGe HBT is more suitable for low-temperature operation than the Si BJT, because of its high current gain and excellent frequency response at low temperatures. In previous work [22], $M-1$ was observed to increase exponentially with cooling, and based on this observation, it was suggested that SiGe HBT's might not be suitable for low-temperature digital applications requiring higher $V_{\rm CB}$, because of the increased current gain and $M-1$ [22]. To clarify this issue, the standard devices with a double-collector implant which are best suited for high-speed digital applications were measured over the temperature range of 80–300 K. Fig. 15 shows the low-temperature $M-1$ data versus collector-base voltage for a typical high-N_C SiGe HBT, and Fig. 16 shows the $M-1$ data as a function of 1000/T for two standard SiGe HBT's with slightly different Ge and doping profiles. Fig. 17 shows the current gain as a function of 1000/T corresponding to the data in Figs. 15 and 16. In contrast to the previous observations of a strongly exponential increase of $M-1$ with cooling, the increase of $M-1$ with cooling is much weaker, particularly below 147 K. The difference in temperature sensitivity is not due to any Ge effect, but instead is attributed to the higher collector doping

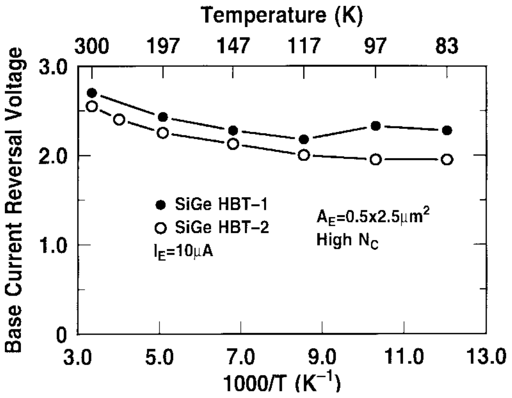

Fig. 18. Measured base current reversal voltage versus 1000/T for two SiGe HBT's with different Ge profiles.

level in the device measured in this study than in the devices used in [22]. Such a weaker dependence of $M-1$ at higher collector doping was indeed observed in [22] in devices with collector doping levels lower than the standard device in this technology. Therefore the reduced temperature dependence of $M-1$ with cooling at high collector doping alleviates the power supply limit posed by the base current reversal voltage, which was previously projected to threaten low-temperature operation of scaled devices featuring high collector doping [22]. The measured base current reversal voltage is above 1.9 V for all of the devices at $I_E = 10$ μA at all temperatures of interest, as shown in Fig. 18, which is sufficient for stable bipolar and BiCMOS logic operation. Our results suggest that impact ionization does not pose a difficulty for the application of SiGe HBT's in BiCMOS logic circuits at low temperatures.

V. CONCLUSIONS

We have measured the collector-base junction avalanche multiplication factor $(M-1)$ using a novel technique in a production-quality SiGe HBT technology. The technique allows the separation of the Early effect and avalanche multiplication effect for the first time, and safe measurement at practical operational current densities for RF circuit applications. Measurements on devices with different collector doping levels indicate that $M-1$ needs to be modeled as a function of current density to accurately predict distortion in circuit simulation. An apparent decrease of the impact ionization rate is observed in SiGe HBT's at high V_{CB} when the contributions of secondary holes are important. A lower $M-1$ in SiGe HBT's results at high V_{CB} due to the population of high energy holes at the base side of the CB-SCR where the Ge content peaks, as confirmed by 2-D energy balance simulation. In contrast to previous reports, we observe a slowdown of the increase in $M-1$ with cooling and a higher than 1.9 V base current reversal CB voltage for all the HBT's, which demonstrates the suitability of SiGe HBT for low-temperature applications.

ACKNOWLEDGMENT

The wafers were fabricated at IBM Microelectronics, East Fishkill, NY. The authors are indebted to D. Harame, S. Subbanna, and B. Meyerson for their support of this work, as well as G. Hurkx for helpful comments on their earlier avalanche multiplication work.

REFERENCES

[1] P. M. Solomon and D. D. Tang, "Bipolar circuit scaling," in *Tech. Dig. ISSCC*, 1979, p. 86.
[2] P. F. Lu and T. C. Chen, "Collector-base junction avalanche effects in advanced double-poly self-aligned bipolar transistors," *IEEE Trans. Electron Devices*, vol. 36, pp. 1182–1188, June 1989.
[3] P. R. Gray and R. G. Meyer, *Analysis and Design of Analog Integrated Circuits*, 3rd ed. New York: Wiley, 1993.
[4] S. Narayanan, "Transistor distortion analysis using volterra series representation," *Bell Syst. Tech. J.*, vol. 40, 1967.
[5] L. C. N. de Vreede, W. van Noort, H. F. F. Jos, H. C. de Graaff, J. W. Slotboom, and J. L. Tauritz, "Optimum dimensions of the epilayer for third-order intermodulation distortion," in *Proc. IEEE BCTM*, 1998, pp. 168–171.
[6] H. C. de Graaff and W. J. Klosterman, *The Mextram Bipolar Transistor Model*, Philips Research Laboratories, 1994. The Mextram model including avalanche multiplication is available in many SPICE or SPICE-like simulators such as Smart-SPICE from Silvaco International.
[7] G. F. Niu, J. D. Cressler, U. Gogineni, and D. L. Harame, "Collector-base junction avalanche multiplication effects in advanced UHV/CVD SiGe HBT's," *IEEE Electron Device Lett.*, vol. 19, pp. 288–290, Aug. 1998.
[8] D. L. Harame, J. H. Comfort, J. D. Cressler, E. F. Crabbé J. Y. C. Sun, B. S. Meyerson, T. Tice, "Si/SiGe epitaxial-base transistors—Part I: Materials, physics, and circuits," *IEEE Trans. Electron Devices*, vol. 42, pp. 469–482, Mar. 1995.
[9] D. C. Ahlgren, G. Freeman, S. Subbanna, R. Groves, D. Greenberg, J. Malinowski, D. Nguyen-Ngoc, S. J. Jeng, K. Stein, K. Schonenberg, D. Kiesling, B. Martin, S. Wu, D. L. Harame, and B. Meyerson, "A SiGe HBT BiCMOS technology for mixed signal RF applications," in *Proc. IEEE BCTM*, 1997, pp. 195–198.
[10] MEDICI, 2-D Semiconductor Device Simulator, version 4.0, *Tech. Model. Assoc.*, Palo Alto, CA, 1997.
[11] G. F. Niu, W. E. Ansley, S. Zhang, J. D. Cressler, and R. Grove, "A 2-D numerical simulation methodology for noise figure optimization in UHV/CVD SiGe HBT's," presented at the *IEEE Topical Meet. Silicon Monolithic Integrated Circuits in RF Systems*, Univ. Michigan, Ann Arbor, Sept. 1998.
[12] C. Canali, F. Capasso, R. Malik, A. Neviani, P. Pavan, C. Tedesco, and E. Zanoni, "Measurement of the electron ionization coefficients at low electrical fields in GaAs-based heterojunction bipolar transistors," *IEEE Electron Device Lett.*, vol. 15, pp. 354–356, Sept. 1994.
[13] R. M. Flitcroft, J. R. P. David, P. A. Houston, and C. C. Button, "Avalanche multiplication in GaInP/GaAs single heterojunction bipolar transistors," *IEEE Trans. Electron Devices*, vol. 45, June 1998.
[14] G. F. Niu, J. D. Cressler, and A. J. Joseph, "Quantifying neutral base recombination and the effects of collector-base junction traps in UHV/CVD SiGe HBT's," *IEEE Trans. Electron Devices*, vol. 45, pp. 2499–2504, Dec. 1998.
[15] C. C. McAndrew and L. W. Nagel, "Early effect modeling in SPICE," *IEEE J. Solid-State Circuits*, vol. 31, pp. 136–138, Jan. 1996.
[16] G. Massobrio and P. Antognetti, *Semiconductor Device Modeling with SPICE*, 2nd ed. New York: McGraw-Hill, 1993.
[17] C. T. Kirk, "A theory of transistor cutoff frequency (f_t) fall-off at high current densities," *IEEE Trans. Electron Devices*, vol. ED-9, pp. 164–174, Mar. 1962.
[18] G. E. Bulman, V. M. Robbins, and G. E. Stillman, "The determination of impact ionization coefficients in (100) gallium arsenide using avalanche noise and photocurrent measurements," *IEEE Trans. Electron Devices*, vol. 32, pp. 2454–2466, Nov. 1995.
[19] E. Zanoni, E. F. Crabbé J. M .C. Stork, P. Pavan, G. Verzellesi, L. Vendrame, and C. Canali, "Extension of impact-ionization multiplication coefficient measurements to high electric fields in advanced Si BJT's," *IEEE Electron Device Lett.*, vol. 14, pp. 69–71, Feb. 1993.
[20] J. Singh, "A theoretical study of electron impact ionization in pesudomorphic InGaAs on GaAs and InP substrates," presented at the *Int. Symp. Gallium Arsenide and Related Compounds*, Sept. 23–26, 1991.
[21] K. W. Eisenbeiser, J. R. East, J. Singh, W. Li, and G. I. Haddad, "Breakdown voltage improvement in strained InGaAs/GaAs FET's," *IEEE Electron Device Lett.*, vol. 13, pp. 421–423, Aug. 1992.
[22] P. F. Lu, "Low-temperature avalanche multiplication in the collector-base junction of advanced n-p-n transistors," *IEEE Trans. Electron Devices*, vol. 37, pp. 762–768, June 1990.

Guofu Niu (M'98) was born in Henan, China, in December 1971. He received the B.S., M.S. and Ph.D. degrees in electrical engineering all from Fudan University, China, in 1992, 1994, and 1997, respectively. His doctoral research concerned the development of 2-D numerical simulator and physical models for SiGe heterostructure MOSFET's.

In December 1995, he joined the City University of Hong Kong, where he worked on the application of network parallel computing in electronics CAD, and the circuit simulation of switched-current oscillators and quantum effect programmable logic gates utilizing resonant tunneling devices. In May 1997, he joined Auburn University, Auburn, AL, where he has been working on SiGe RF and microwave bipolar and FET devices and circuits, low-frequency and broadband noise, device reliability, nuclear and space radiation effects, and TCAD as a Postdoctoral Research Fellow. He has authored and coauthored more than 20 technical journal papers and more than 20 conference papers in the area of microelectronic devices and circuits.

Dr. Niu served on the Program Committee of Asia-South-Pacific Design Automation Conference (ASP-DAC) in 1997, and served as a Technical Reviewer for IEEE ELECTRON DEVICE LETTERS, IEEE TRANSACTIONS ON ELECTRON DEVICES, IEEE JOURNAL ON SOLID STATE CIRCUITS, and *Solid-State Electronics.*

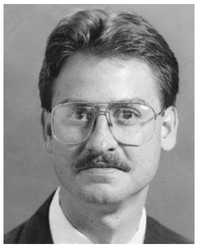

John D. Cressler (S'86–SM'91) received the B.S. degree in physics from the Georgia Institute of Technology, Atlanta, in 1984, and the M.S. and Ph.D. degrees in applied physics from Columbia University, New York, NY, in 1987 and 1990, respectively.

From 1984 to 1992, he was on the research staff at the IBM T. J. Watson Research Center, Yorktown Heights, NY, where he worked in the Semiconductor Science and Technology Department on submicron Si and SiGe bipolar technology. His research interests at IBM included the physics and design of both ion-implanted and epitaxial Si and SiGe-base bipolar transistors and circuits, and particularly the operation and understanding of such devices at cryogenic temperatures. In addition to his responsibilities while at IBM, he was an Adjunct Professor of Mathematics at Western Connecticut State University, Danbury, from 1987 to 1990, as well as an Adjunct Assistant Professor of Electrical Engineering at Columbia University from 1990 to 1992. In 1992, he left the IBM Research Division to join the faculty of Auburn University, Auburn, AL. His research interests include SiGe HBT's and FET's, radiation effects, cryogenic electronics, SiC devices, RF/microwave circuits, reliability, noise, device simulation, and compact circuit modeling. He is currently Professor of Electrical Engineering and Assistant Director of the Alabama Microelectronics Science and Technology Center (AMSTC), a multidisciplinary, state-funded research center, and Director of the Cryogenic Electronics Laboratory within the AMSTC. He has published over 145 technical papers related to his research and written three book chapters.

Dr. Cressler received five awards from the IBM Research Division. He served on the Technical Program Committee for the ISSCC (1992–1998), the BCTM (1995-present), and the IEDM (1996–1997) conferences. He was the Technical Program Chairman of the 1998 ISSCC, and is currently Chair of the Device Physics subcommittee of the BCTM. He was appointed an IEEE Electron Devices Society Distinguished Lecturer in 1994. He was awarded the 1996 C. Holmes MacDonald National Outstanding Teacher Award by Eta Kappa Nu, the 1996 Auburn University Alumni Engineering Council Research Award, and the 1998 Birdsong Merit Teaching Award. He received the Office of Naval Research Young Investigator Award in 1994 for his SiGe research program. He has served as a consultant to IBM, Analog Devices, Westinghouse, ITRI/ERSO (Taiwan), Teltech, the National Technological University, and Commercial Data Servers. He is currently an Associate Editor of IEEE JOURNAL OF SOLID-STATE CIRCUITS.

Shiming Zhang (S'99) was born in Beijing, China, in 1968. He received the B.E. degree in electrical engineering from Beijing Polytechnic University, China, in 1992. He is currently pursuing the M.S. degree in the electrical engineering department, Auburn University.

From 1992 to 1997, he worked on SiGe HBT in Beijing Polytechnic University as a Research Assistant. His main research interest is the RF and microwave characterization of SiGe HBT.

Usha Gogineni (S'97) was born in Bhimavaram, India. She received the B.Tech. degree in electronics and communication engineering from Regional Engineering College, Warangal, India, in 1996, and the M.S. degree in electrical engineering from Auburn University, Auburn, AL. Her graduate research was on the reliability of silicon-germanium heterojunction bipolar transistors (HBT's). She has published one journal and three conference papers related to the effects of emitter-base reverse-bias stress and avalanche multiplication effects in UHV/CVD SiGe HBT's. Her research interests lie in the areas of HBT physics, device characterization, low-temperature electronics, and low-frequency noise.

David C. Ahlgren received the B.A. degree from DePauw University, Greencastle, IN, in 1973 and the Ph.D. degree in chemical physics from The University of Michigan, Ann Arbor, in 1979.

He joined IBM in Hopewell Junction, NY, in 1979 conducting semiconductor process development. His early work was in the area of silicon defects resulting from ion implantation and isolation stress, as well as process integration issues which lead to the development and subsequent production of IBM's first double polyslilicon bipolar technology in 1983. In 1989 his attention turned to Si/SiGe HBT's as the next step in the advancement of IBM's bipolar mainframe semiconductor technology. His early device studies, process technology work, and semiconductor production experience has lead him into his current role in the Advanced Semiconductor Technlology Center as a Senior Engineer in device and process development of high-performance Si/SiGe BiCMOS technology and its introduction into manufacturing. He has published over 30 papers and holds eight patents in semiconductor device and process technology.